Mechanism of Effective Quenching of Calcein Fluorescence by Iron.
Ab initio study

Valentinas Černiauskas [a] , Alytis Gruodis, Raminta Rodaitė-Riševičienė, Gintautas Saulis

Department of Biology, Vytautas Magnus University,

8 Vileikos str., Kaunas, Lithuania

Abstract. Geometry of the associate of the calcein and iron ion was determined using density functional CAM-B3LYP method. A stable associate was obtained only as set of a two calcein molecules and iron ion. The nature of the calcein luminescence extinguished by Fe^{2+} ions is explained by the formation of low-lying eight additional electronic states, when the transitions from the above states to the ground states are completely forbidden due to the heavy metal Fe^{2+} effect. Energetical scheme (in the form of Jablonski diagram) is illustrated by plots of charge redistribution between one-particle states which are related to spectrometric states.

Introduction

Cell electroporation represents the process when the permeability of the cell plasma membrane temporary increases due to strong electrical field pulse (up to 300 kV/cm). As an invasive method, cell electroporation is widely used in cell biology, biotechnology, and medicine [1,2]. The application of high voltage in the electrolyte medium, despite other electrolytic reactions, involves the oxidation of the metal of anode. For this reason, the anode begins to melt [3].

Metal ions emitted from electrodes can react with fluorescent molecules and reduce their fluorescence intensity. One of the most popular materials used in the production of electrodes and applied to cell electroporation is stainless steel. Usage of high-voltage pulses creates a substantial number of iron ions (Fe^{2+} and Fe^{3+}) from the anode [4].

Calcein - a well-known derivative of fluorescein - belongs to the class of fluorescent dyes. It is widely used for the determination of the permeabilization of biological membranes [5,6] including cell electroporation studies [7,8].

Influence of iron ions on the intensity of calcein fluorescence was observed in various media, e.g. HEPES-buffered saline, cytoplasm-like solution or serum [9,10]. The results of this work may be useful in evaluating the effectiveness of cell electroporation [11].

The aim of this work was to study *in silico* the structure and energetical properties of calcein derivatives in surroundings where significant amounts of Fe^{2+} are present:

a) to determine the most probable geometry of associates consisting of calcein molecule and iron ion Fe^{2+};
b) to explain the mechanism of quenching of calcein luminescence.

1. Literature review

Fluorescence is a molecular process of spontaneous emission of radiation, which is not related to the thermal equilibrium with its environment [12-15]. Emission could occur from electronically excited state. Excitation must be provided by external source, for example, laser, LED etc. in case if excitation wavelength corresponds to the wavelength interval of absorption band.

Fluorophores (fluorescent probes) are extremally stable molecular derivatives that absorb light of a certain wavelength and emit it at longer wavelengths - so called Stokes shift occurs [13,15]. Main reason of such phenomenon is related to the processes of internal conversion when non-radiative transitions occur [14].

The usage of fluorescent probes allows solving the visualization problems: fluorescent probes have a high contrast to dark background, high sensitivity and specificity. Fluorophores are usually minimally-invasive compounds that can be present in live cells for real-time exposition without cell fixation [16].

Fluorescence imaging belongs to one of the most important non-invasive methods in contemporary biological scien-

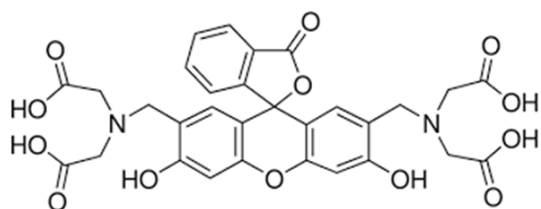[a]Corresponding author, email: valentinas.cernis@gmail.lt
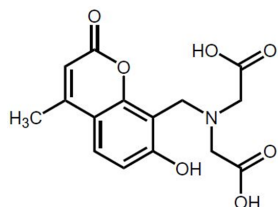
Fig. 1. Calcein green.

Fig. 2. Calcein blue.

ces [13]. High sensitivity of the method allows precise usage for medical needs, working with unknown biological structures [16]. From a physical point of view, several factors are important for occurrence of the fluorescence images:

i)   quantum energy and intensity of excitation source;
ii) stability and quantum efficiency of fluorophore [17];
iii) presence of quenchers and agents of resonant energy transfer [18];
iv) presence of (photo)oxidation reagents in the medium.

2. Chemical structures

Calcein green [19] and calcein blue [20] are dyes for visualization purposes *in vitro* with high luminescence yield - see

Figs. 1-2. Due to high molecular stability, calcein plays a role of short-term label in the cell with excitation and emission at 495/515 nm (2.5/2.4 eV), respectively [21].

Acetoxymethyl (AM) esters of calcein green and calcein blue are non-fluorescent compounds, which can freely pass though the cellular membrane into live cells. The active esterases within live cells cleave AM group and calcein-AM is transformed into a bright fluorescent form – calcein, which is membrane-impermeant [22]. Such an approach is used to recognize viable cells because dead cells either do not have the intact plasma membrane or do not contain active enzyme esterases that can hydrolyze calcein–AM.

3. Quantum chemistry simulations

Quantum-chemical structure simulations were performed with *Gaussian16* package [23]. Molecular geometry was optimized by density functional CAM-B3LYP method using a 6-31G(d) base with polarizing d functions without environmental impact. Fig. 3 represents the model derivative M1 corresponding to a complex of two calcein molecules and an Fe^{2+} ion. In order to simplify the ground state energy minimization procedure, calcein structure has been used without long-chain substitutions, but it is still called as "calcein". Three projections allow to imagine the nature of bonding through the iron ion. Due to the sp^2 hybridization, the bonding is formed in a plane containing a calcein phenyl ring with carbonyl. The intermolecular bridge is formed as a double behaviour of co-ordinate bonds $[..C=O-Fe^{2+}-O=C..]$ and $[..C=O\rightarrow Fe^{2+}\leftarrow O=C..]$.
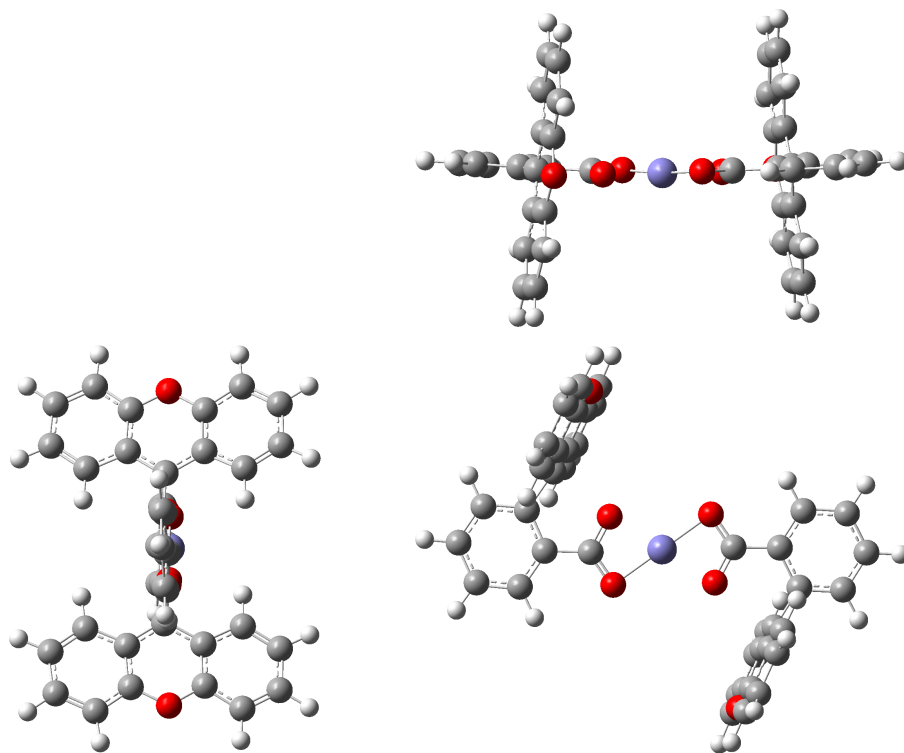

Fig. 3. A model derivative M1 as the complex of two calcein molecules and an Fe^{2+} ion (at centrum). X0Z, X0Y, Y0Z projections.

Table 1. Electronic transitions of simulated absorption spectrum of model compound M1.
*Gaussian16*[23], semiempirical method TD, only singlets included.

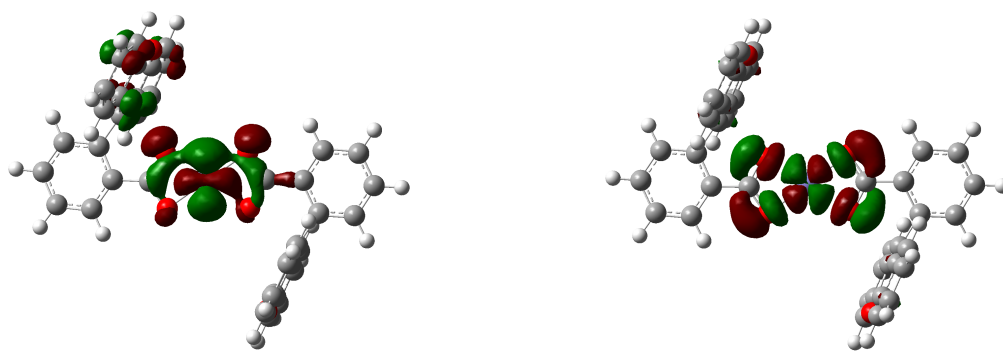| Electronic transition	Energy, eV	Oscillator strength	One-particle transitions	Coef.	Figs.
$E_0 \rightarrow E_1$	0.495	0.000	167B→170B	-0.43	
			167B→177B	-0.42	
			167B→179B	-0.70	4
$E_0 \rightarrow E_2$	0.571	0.000	**157A→174A**	-0.53	5
			161A→174A	-0.51	5
			164B→182B	-0.53	5
			167B→182B	-0.40	
$E_0 \rightarrow E_3$	0.579	0.000	164B→181B	-0.63	
			167B→181B	-0.76	6
$E_0 \rightarrow E_4$	0.949	0.000	157A→174A	0.42	
			161A→174A	-0.49	7
			164B→182B	0.45	
			167B→182B	-0.44	
$E_0 \rightarrow E_5$	1.075	0.000	164B→170B	-0.40	
			164B→179B	-0.64	8
$E_0 \rightarrow E_6$	1.569	0.000	**164B→181B**	0.70	9
			167B→181B	-0.59	
$E_0 \rightarrow E_7$	1.893	0.000	**157A→174A**	-0.66	10
			164B→182B	0.57	
$E_0 \rightarrow E_8$	2.220	0.000	168A→170A	-0.62	
			165B→168B	0.64	11

The electronic excitations were calculated by means of semi-empirical TD method for singlets only (number of states is equal to 10). Table 1 shows the simulated electron absorption spectrum of the model compound M1. Parameters of spectroscopic states (excitation energy and oscillator strength) as well as corresponding one-particle transitions are presented in order to estimate the population of excited states from lowest excited E_1 up to E_8. Set of transitions could be divided into three groups: transitions in the band group about 0.5 eV, band group about 1 eV, band group in region 1.5÷2 eV. Other transitions into higher states are not significant. The limit of about 2 eV was chosen because the fluorescence of the iron-free calcein derivatives is observed from the state about 2.31 eV, and the iron ions quench that luminescence very effectively. In this case, eight excited electronic states below 2.3 eV are related to the quenching processes.

Typically, the eight lowest transitions are completely forbidden (oscillator strength of transition is equal to zero). Hence, a radiative transition (fluorescence emission) is impossible, only internal relaxation processes take place. The molecular state at 2.31 eV is not populated, and the state E_1 at 0.49 eV must be titled as the lowest excited singlet state. Since the transition $E_0 \rightarrow E_1$ is forbidden (and also $E_1 \rightarrow E_0$), there is no luminescence.

Tables 4÷11 show the redistributions of electronic clouds by population of excited states E_n, n=1÷8. All charge redistributions are depicted in the framework of MO related to the one-particle transition. Most important one-particle transition could be divided into three groups.

For low lying states E_n, n=1,2,3, (see Figs. 4÷6), two types of intermolecular redistribution occur. Firstly, transition between MO 167B→179B (from left to right calcein, see
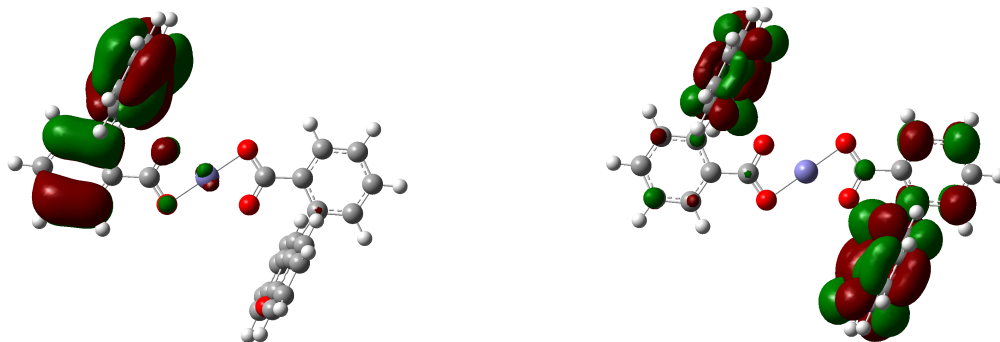
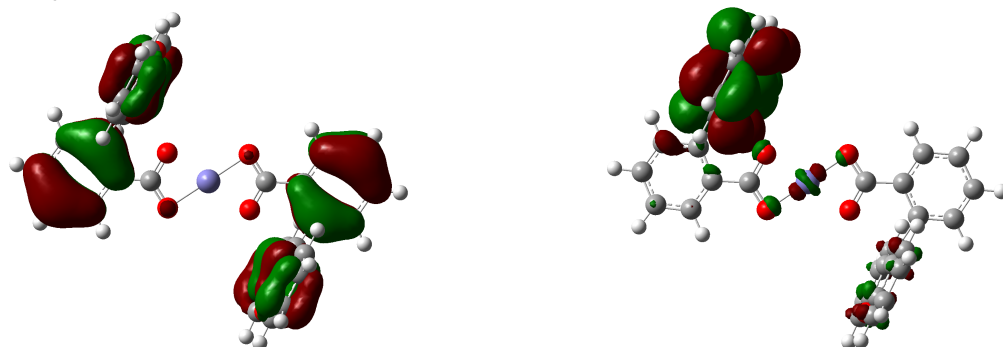

Charge redistribution between MO: **167B→179B**
Fig. 4. Electronic transition $E_0 \rightarrow E_1$, transition energy 0.495 eV, oscillator strength 0.000.
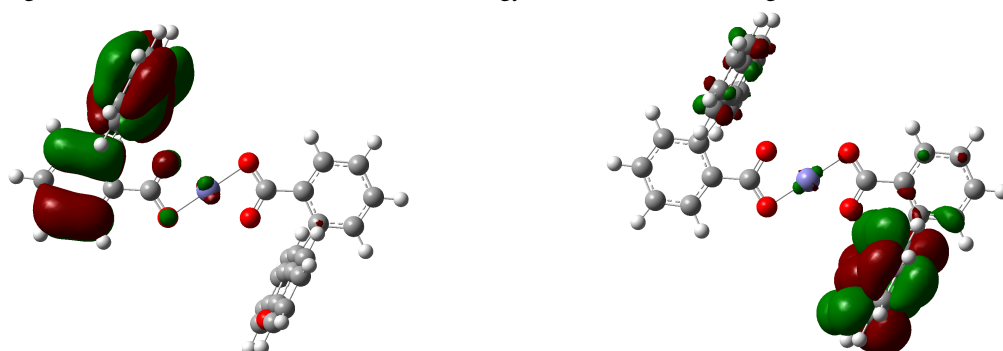
Charge redistribution between MO: **157A→174A**
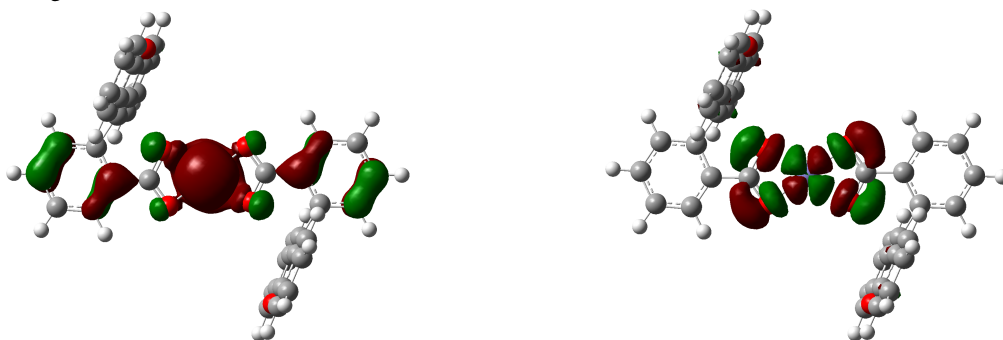
Charge redistribution between MO: **161A→174A**

Charge redistribution between MO: **164B→182B**

Fig. 5. Electronic transition $E_0 \rightarrow E_2$, transition energy 0.571 eV, oscillator strength 0.000.

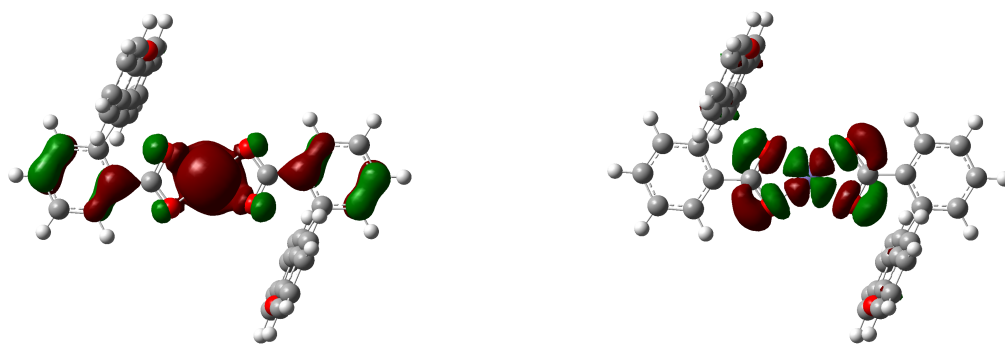
Charge redistribution between MO: **167B→181B**

Fig. 6. Electronic transition $E_0 \rightarrow E_3$, transition energy 0.579 eV, oscillator strength 0.000.

Fig. 4) as $\pi \rightarrow \pi*$ transition is typical for such type redistributions. Iron ion plays the role of the mediator in order to establish the bridge behaviour for inter-fragmental redistribution. The same type is realized for transition between MO 167B→181B (from left calcein to right calcein, see Fig. 6). Secondly, transitions between MO 157A→174A and 161A→174A (from iron ion and oxygen-carbon atoms in near surrounding to iron ion with neighbour oxygens, see Fig. 5) must be treated as mixed transition with $n \rightarrow \pi*$ impact (n electrons from oxygen atoms).

For low intermediate states E_n, n=4,5,6, (see Figs. 7÷9), two types of intermolecular redistribution occur. Firstly, tran-
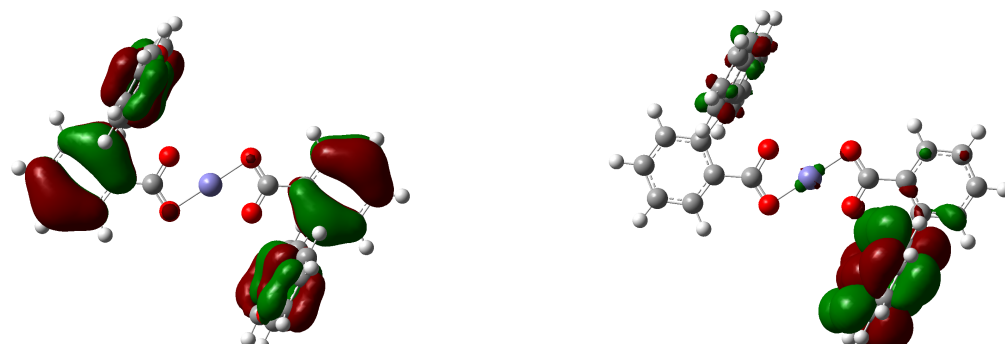
Charge redistribution between MO: **161A→174A**

Fig. 7. Electronic transition $E_0 \rightarrow E_4$, transition energy 0.949 eV, oscillator strength 0.000.
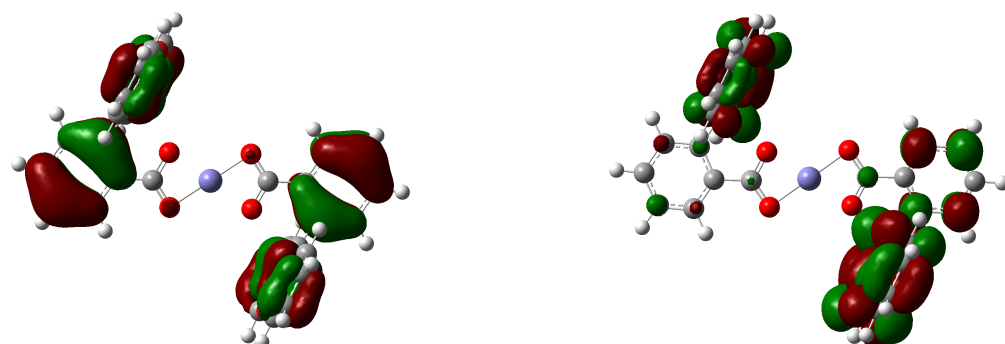
Charge redistribution between MO: **164B→179B**

Fig. 8. Electronic transition $E_0 \rightarrow E_5$, transition energy 1.075 eV, oscillator strength 0.000.

Charge redistribution between MO: **164B→181B**

Fig. 9. Electronic transition $E_0 \rightarrow E_6$, transition energy 1.569 eV, oscillator strength 0.000.

sition between MO 164B→179B (from left to right calcein, see Fig. 8) as $\pi \rightarrow \pi^*$ transition is typical for such type redistributions. The same type is realized for transition between MO 164B→181B (from left calcein to right calcein, see Fig. 9). It is necessary to point out that full CT transition is not realized in both cases. Secondly, transitions between MO 161A→174A (from iron ion and oxygen-carbon atoms in plane surface to iron ion with neighbour oxygens in the same plane surface, see Fig. 7) must be treated as mixed transition with $n \rightarrow \pi^*$ impact.

For high energy states E_n, n=7,8, (see Figs. 10÷11), two types of intermolecular redistribution occur. Firstly, transitions between MO 157A→174A (from iron ion and oxygen-carbon atoms in plane surface to iron ion with neighbour oxygens in the same plane surface, see Fig. 10) must be treated

as mixed transition with $n \rightarrow \pi^*$ impact.

Secondly, new type of charge redistribution occurs for transition between MO 165B→168B (from plane surface containing two calcein molecules to right calcein, see Fig. 11). This transition of mixed type is forbidden due to orthogonality condition (fragments are perpendicular).

Fig. 12 represents Jablonski diagram explaining the quenching effect of calcein fluorescence due to iron ions. For iron-free calcein (left diagram), absorption and luminescence are present as radiative transitions $S_0 \rightarrow S_1$ and $S_1 \rightarrow S_0$, respectively. Quenching of luminescence is absent. For M1 compound containing Fe^{2+} (right diagram), transitions $S_n \rightarrow S_0$, n=1÷8, are forbidden (oscillator strengths are equal to zero), luminescence (emission) is impossible. According
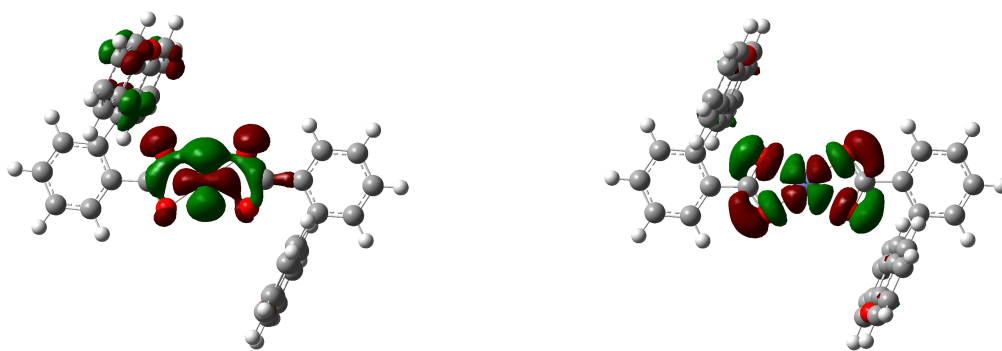
Charge redistribution between MO: **157A→174A**

Fig. 10. Electronic transition $E_0{\rightarrow}E_7$, transition energy 1.893 eV, oscillator strength 0.000.
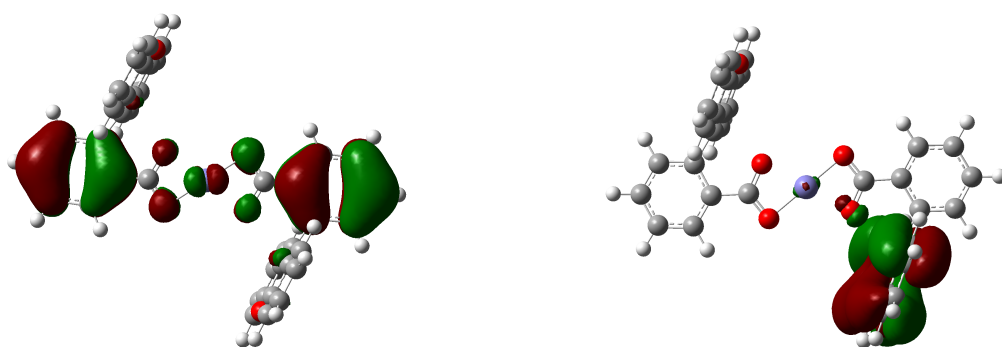
Charge redistribution between MO: **165B→168B**

Fig. 11. Electronic transition $E_0{\rightarrow}E_8$, transition energy 2.220 eV, oscillator strength 0.000.
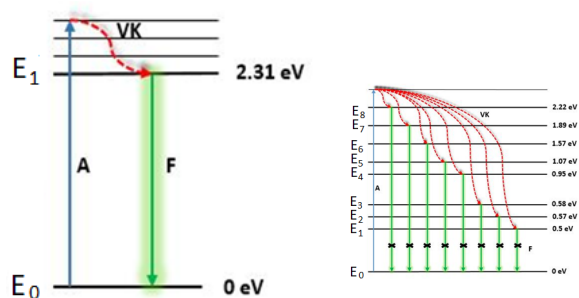

Fig. 12. Jablonski diagram for iron-free calcein (left, allowed emission) and M1 compound (right, forbidden emission).

to Franck–Condon principle, depopulation of the excited states could be realized through non-radiative processes of internal conversion.

It is necessary to point out that the state E_1 (most important for quenching process) is present in infra-red region (2.5μm/0.5 eV).

4. Conclusions

The geometry of calcein and iron ion associate was investigated by simulations using CAM-B3LYP/6-31G(d) method.

The stable structure was obtained only for associate consisting of two calcein molecules and the iron ion.

The nature of calcein luminescence extinguishing with Fe^{2+} ions was explained by the formation of eight additional electronic states, when transitions from excited states to the ground state are completely forbidden due to the heavy metal (Fe^{2+}) effect.

Three types of charge redistribution between MO were established:

a) intermolecular between two calcein molecules;
b) "intramolecular" in near Fe^{2+} surrounding including neighbour oxygen atoms;
c) intermolecular between two perpendicular plane surfaces from calcein to calcein.

References

1. Kinosita Kazuhiko ir Tsong Tian Yow. Formation and resealing of pores of controlled sizes in human erythrocyte membrane. – *Nature* 268 (1977) 438–441. – DOI 10.1038/268438a0.

2. Yarmush Martin L., Goldberg Alexander, Ssersa Gregor, Kotnik Tadej ir Miklavčič Damijan. Electroporation-Based Technologies for Medicine: Principles, Applications, and Challenges. – *Annual Review of Biomedical Engineering* 16(1) (2014) 295-320. – DOI 10.1146/annurev-bioeng-071813-104622. – <http://www.annualreviews.org/doi/10.1146/annurev-bioeng-071813-104622>, accessed 2017 10 02.

3. Samaranayake Chaminda P. ir Sastry Sudhir K. Electrode and pH effects on electrochemical reactions during ohmic heating. – *Journal of Electroanalytical Chemistry* 577(1) (2005) 125-135. – DOI 10.1016/j.jelechem.2004.11.026.

4.   Raminta Rodaitė-Riševičienė, Rita Saulė, Valentinas Snitka, Gintautas Saulis. Release of iron ions from the stainless steel anode occurring during high-voltage pulses and its consequences for cell electroporation technology. – *IEEE Transactions on Plasma Science* 42(1) (2014) 249–254. – DOI 10.1109/TPS.2013.2287499.

5.   Sara G. Hovakeemian, Runhui Liu, Samuel H. Gellman and Heiko Heerklotz. Correlating antimicrobial activity and model membrane leakage induced by nylon-3 polymers and detergents. – *Soft Matter* 11 (2015) 6840–6851. – DOI 10.1039/C5SM01521A.

6.   Poonam Tyagi, Madhuri Singh, Himani Kumari, Anita Kumari, Kasturi Mukhopadhyay. Bactericidal Activity of Curcumin I Is Associated with Damaging of Bacterial Membrane. – *PLoS ONE* 10(3) (2015) e0121313. – DOI 10.1371/journal.pone.0121313.

7.   P.J. Canatella, J.F. Karr, J.A. Petros, M.R. Prausnitz. Quantitative study of electroporation-mediated molecular uptake and cell viability. – *Biophys. J.* 80 (2001) 755–764.

8.   M.R. Prausnitz, J.D. Corbett, J.A. Gimm, D.E. Golan, R. Langer, J.C. Weaver. Millisecond measurement of transport during and after an electroporation pulse. – *Biophys. J.* 68 (1995) 1864–1870).

9.   William Breuer, Silvina Epsztejn, Phina Millgram, Ioav Z. Cabantchik, Transport of iron and other transition metals into cells as revealed by a fluorescent probe. – *American Journal of Physiology – Cell Physiology* 268 (1995) C1354-C1361. – DOI 10.1152/ajp-cell.1995.268.6.C1354.

10. Aktar Ali, Qi Zhang, Jisen Dai & Xi Huang. Calcein as a fluorescent iron chemosensor for the determination of low molecular weight iron in biological fluids. – *BioMetals* 16(2) (2003) 285–293. – DOI 10.1023/A:1020642808437.

11. Wei Lee Leong, Jagadese J. Vittal. Synthesis and characterization of metal complexes of Calcein Blue: Formation of monomeric, ion pair and coordination polymeric structures. – *Inorganica Chimica Acta* [online] 362(7) (2009) 2189-2199. – DOI 10.1016/j.ica.2008.09.049. – <http://dx.doi.org/10.1016/j.ica.2008.09.049>, accessed 2017 09 06.

12. Joseph R. Lakowicz. Principles of Fluorescence Spectroscopy. Third Edition. – Springer, 2006.

13. Bernard Valeur, Mário Nuno Berberan-Santos. Molecular Fluorescence: Principles and Applications, Second Edition. – Wiley-VCH Verlag GmbH & Co. KGaA., 2013.

14. An Introduction to Fluorescence Spectroscopy – PerkinElmer, Inc. , 2000.

15. Bernard Valeur, Mário N. Berberan-Santos. A Brief History of Fluorescence and Phosphorescence before the Emergence of Quantum Theory. – *Journal of Chemical Education* 88 (2011) 731-738. – dx.doi.org/10.1021/ed100182h.

16. Hellen C. Ishikawa-Ankerhold, Richard Ankerhold and Gregor P. C. Drummen. Advanced fluorescence microscopy techniques-FRAP, FLIP, FLAP, FRET and FLIM. – *Molecules* 17(4) (2012) 4047–4132. – DOI 10.3390/molecules17044047.

17. David M. Jameson. Introduction to Fluorescence. – Teylor/Francis Group LLc, 2014.

18. Nicholas J. Turro and V. Ramamurthy. Modern Molecular Photochemistry of Organic Molecules. – Sausalito: University Science Books, 1991.

19. BURROWS, Sean M., REIF, Randall D. ir PAPPAS, Dimitri. Investigation of photobleaching and saturation of single molecules by fluorophore recrossing events. – *Analytica Chimica Acta* 598(1) (2007) 135–142. – DOI 10.1016/j.aca.2007.07.026.

20. Seto D., Maki T., Soh N., Nakano K., Ishimatsu R., Imato T. A simple and selective fluorometric assay for dopamine using a calcein blue-Fe2+ complex fluorophore. – *Talanta* 94 (2012) 36-43. – DOI 10.1016/j.talanta.2012.02.025. <http://dx.doi.org/10.1016/j.talanta.2012.02.025>, accessed 2017 11 15.

21. Allen T. M. ir Cleland L. G. Serum-induced leakage of liposome contents. – *BBA - Biomembranes* 597(2) (1980) 418–426. – DOI 10.1016/0005-2736(80)90118-2.

22. Bratosin D., Mitrofan L., Palii C., Estaquier J., Montreuil J. Novel fluorescence assay using calcein-AM for the determination of human erythrocyte viability and aging. – *Cytometry A* 66(1) (2005) 78–84. – DOI 10.1002/cyto.a.20152.

23. Gaussian 16, Revision B.01, M. J. Frisch, G. W. Trucks, H. B. Schlegel, G. E. Scuseria, M. A. Robb, J. R. Cheeseman, G. Scalmani, V. Barone, G. A. Petersson, H. Nakatsuji, X. Li, M. Caricato, A. V. Marenich, J. Bloino, B. G. Janesko, R. Gomperts, B. Mennucci, H. P. Hratchian, J. V. Ortiz, A. F. Izmaylov, J. L. Sonnenberg, D. Williams-Young, F. Ding, F. Lipparini, F. Egidi, J. Goings, B. Peng, A. Petrone, T. Henderson, D. Ranasinghe, V. G. Zakrzewski, J. Gao, N. Rega, G. Zheng, W. Liang, M. Hada, M. Ehara, K. Toyota, R. Fukuda, J. Hasegawa, M. Ishida, T. Nakajima, Y. Honda, O. Kitao, H. Nakai, T. Vreven, K. Throssell, J. A. Montgomery, Jr., J. E. Peralta, F. Ogliaro, M. J. Bearpark, J. J. Heyd, E. N. Brothers, K. N. Kudin, V. N. Staroverov, T. A. Keith, R. Kobayashi, J. Normand, K. Raghavachari, A. P. Rendell, J. C. Burant, S. S. Iyengar, J. Tomasi, M. Cossi, J. M. Millam, M. Klene, C. Adamo, R. Cammi, J. W. Ochterski, R. L. Martin, K. Morokuma, O. Farkas, J. B. Foresman, and D. J. Fox, Gaussian, Inc., Wallingford CT, 2016.